

# Cerenkov-Type Second-Harmonic Generation in Two-Dimensional Nonlinear Photonic Structures

Solomon Mois Saltiel, Yan Sheng, Noa Voloch-Bloch, Dragomir N. Neshev, Wieslaw Krolikowski, Ady Arie, Kaloian Koynov, and Yuri S. Kivshar

**Abstract**—We study the Cerenkov-type second-harmonic generation in several different two-dimensional nonlinear photonic structures formed in birefringent crystals with the 3m symmetry. Depending on the degree of birefringence, we observe either single or double Cerenkov-like second-harmonic rings. We discuss the properties of these parametrically generated rings and show that their sixfold azimuthal modulation is associated with the hexagonal symmetry of the individual ferroelectric domains.

**Index Terms**—Cerenkov phase-matching, nonlinear diffraction, quasi-phase-matching, second-harmonic generation.

## I. INTRODUCTION

IT IS well known that second-harmonic generation (SHG) can be achieved by many different ways depending on the geometry of the wave phase matching (e.g., birefringence-induced phase matching or quasi-phase matching (QPM), input light polarization (e.g., Type I or Type II), mutual orientation of the wave vectors of interacting waves (collinear or noncollinear), type of the nonlinear media, etc.). Among the most interesting SHG processes is the so-called Cerenkov scheme of SHG [1] named so because of the close analogy with the famous Cerenkov effect in which a particle moving with velocity exceeding the speed of light in the medium emits conical radiation [2]. The Cerenkov frequency doubling represents the type of noncollinear SHG where the second harmonic is generated at an angle with respect to the propagation direction of the fundamental wave. In the case of circular symmetry, the Cerenkov-type SHG leads to a second harmonic emitted in the form of a cone with an axis coinciding with the

Manuscript received April 07, 2009; revised July 23, 2009. Current version published November 06, 2009. This work was supported by the Australian Research Council and Israel Science Foundation (Grant 960/05).

S. M. Saltiel (deceased May 07, 2009) was with the Nonlinear Physics Center and Laser Physics Center, Research School of Physics and Engineering, Australian National University, Canberra, Australia, and also with the Department of Physics, Sofia University “St. Kl. Ohridski”, Sofia, Bulgaria.

Y. Sheng and K. Koynov are with the Max Plank Institute for Polymer Research, Mainz 55128, Germany (e-mail: sheng@mpip-mainz.mpg.de; koynov@mpip-mainz.mpg.de).

N. Voloch-Bloch and A. Arie are with School of Electrical Engineering, Tel-Aviv University, Tel Aviv 69978, Israel (e-mail: noavoloch@gmail.com; ady@eng.tau.ac.il).

D. N. Neshev, W. Krolikowski, and Y. S. Kivshar are with Nonlinear Physics Center and Laser Physics Center, Research School of Physics and Engineering, Australian National University, Canberra ACT 0200, Australia (e-mail: Dragomir.Neshev@anu.edu.au; wzkl11@rsphysse.anu.edu.au; ysk124@rsphysse.anu.edu.au).

Color versions of one or more of the figures in this paper are available online at <http://ieeexplore.ieee.org>.

Digital Object Identifier 10.1109/JQE.2009.2030147

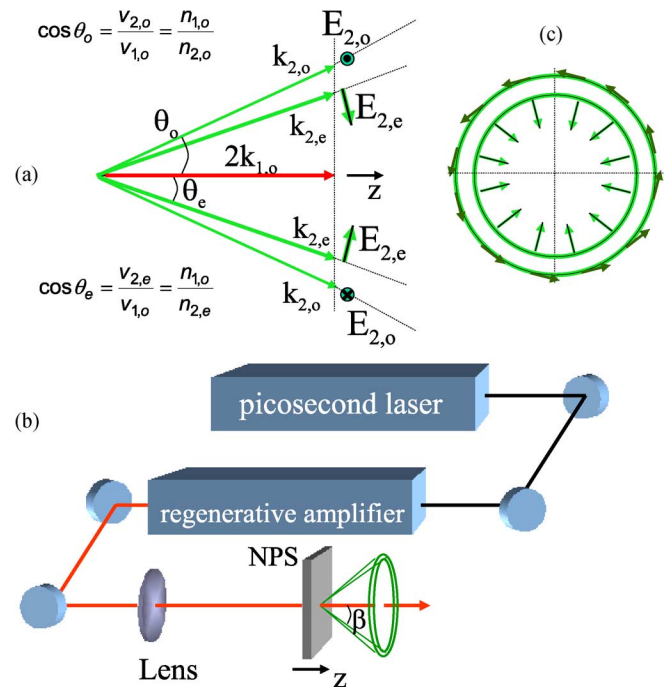


Fig. 1. (a) Phase matching diagram for obtaining Cerenkov type second harmonic in birefringent crystals; (b) Experimental setup: NPS—nonlinear photonic structure formed by spatial modulation of the sign of the nonlinearity; (c) Illustration of polarization properties of the Cerenkov second harmonic rings. Internal ring is radially polarized, the external one—azimuthally.

direction of the fundamental beam. The Cerenkov-type SHG is characterized by the direction of SH emission defined solely by the longitudinal phase matching condition  $k_2 \cos \theta - 2k_1 = 0$ , with  $k_1$ ,  $k_2$  denoting the wave vectors of the fundamental and second-harmonic waves, respectively, and  $\theta$  is the angle of conical emission [see Fig. 1(a)]. Several publications reported the observation of Cerenkov-type SHG in bulk nonlinear media [1], [3], [4]. However, this type of SHG is more often realized in a waveguide geometry [5]–[7].

Nowadays SHG as well as other parametric processes are commonly realized in engineered nonlinear photonic structures with a periodic spatial modulation of the sign of the quadratic nonlinearity. The efficient frequency conversion in such quadratic photonic lattices [8] is achieved by the phase-matching condition via the QPM techniques. It is natural to pose the question about the effect of these structures on the Cerenkov-type SHG processes. In fact, the observation of the Cerenkov-type SHG in one-dimensional periodically poled KTP crystals has been reported in [9]. However, in this particular case the emission was attributed to the second-order

nonlinearity of the domain walls since the symmetry of the crystal does not allow a bulk emission of SH in the investigated geometry. We have recently demonstrated the Cerenkov SH emission via bulk  $\chi^{(2)}$  tensor components in a one-dimensional periodically poled structure in Lithium Niobate crystal [10].

Here we present the results of our systematic study of the Cerenkov SHG in different types of two-dimensional nonlinear photonic structures fabricated in 3m symmetry ferroelectric crystals with periodic, quasi-periodic, and random spatial modulation of the quadratic nonlinearity. In particular, we show that the presence of the modulation of nonlinearity greatly enhances the Cerenkov emission. We demonstrate that the cone angles of the observed Cerenkov SHG rings do not depend on the  $\chi^{(2)}$  modulation patterns, and they are defined only by the bulk indices of refraction.

The paper is organized as follows. In Section II we introduce the photonic structures considered here and also present our experimental results. Section III is devoted to comparison between the different structures and discussion of the specific features of the effects observed in experiments. We discuss in this part the azimuthal intensity modulation of the Cerenkov SH rings and their polarization properties. Finally, Section IV concludes the paper.

## II. EXPERIMENT

The schematic diagram of our experiment is depicted in Fig. 1(b). The fundamental pump beam is derived from a passively mode-locked oscillator followed by a regenerative amplifier, delivering 10 ps, pulses with energy  $\approx 1$  mJ, at 1053 nm and repetition rate of 20 Hz. The beam is directed at normal incidence at the surface of the sample. The beam is loosely focused to a spot size of  $\approx 500 \mu\text{m}$  in the plane of the crystal. After passing through the sample the fundamental beam is blocked by appropriate filters and the emitted second harmonic signal is recorded on a screen placed behind the sample, using a CCD camera.

In this work we study several different two-dimensional nonlinear photonic structures. They include: rectangular and annularly poled structures in stoichiometric  $\text{LiTaO}_3$  [11], [12], decagonal nonlinear photonic quasi-crystal structure [13], and a short-range ordered randomized poled structures in  $\text{LiNbO}_3$  [14], [15]. The ferroelectric domain patterns for all these structures are depicted in the left column of Fig. 2.

The samples have the following design parameters: (a) rectangular periodically poled structures in stoichiometric  $\text{LiTaO}_3$  (RSLT): the dimensions of the basic rectangular cell are  $a = 9.4 \mu\text{m}$  and  $b = 8.5 \mu\text{m}$  [see Fig. 2(a)-left]; (b) annularly poled structures in stoichiometric  $\text{LiTaO}_3$  (ASLT). Consisting of concentric rings of constant thickness with alternating sign of the nonlinearity: the poling period is  $\Lambda = 7.5 \mu\text{m}$  [see Fig. 2(b)-left]; (c)  $\text{LiNbO}_3$  decagonal nonlinear photonic quasi-crystal structure (DQC-LNB is composed of two types of rhombi—the thin one with vertex angles of  $36^\circ$  and  $144^\circ$ , and the thick one with vertex angles of  $72^\circ$  and  $108^\circ$ . The side length of the rhombi is  $c = 13.19 \mu\text{m}$  [see Fig. 2(c)-left]; (d) short-range ordered poled structure in lithium niobate (SRO-LNB), fabricated by a random rotation of basic square

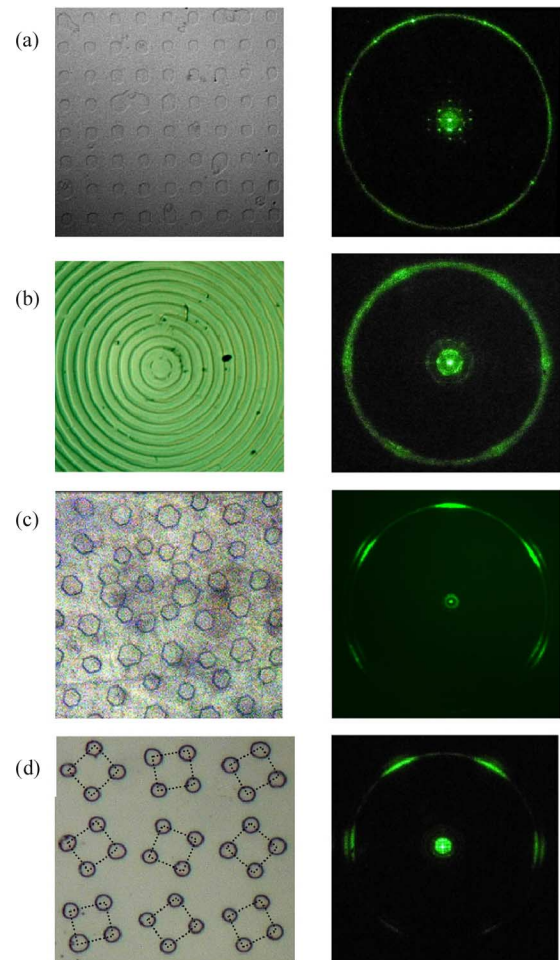


Fig. 2. Visualized poled domains after the etching of the Z surface of nonlinear photonic structures used in the experiment (left) and recorded Cerenkov second harmonic rings (right) in (a) rectangular periodically poled structures in stoichiometric  $\text{LiTaO}_3$  (RSLT); (b) annularly poled structures in stoichiometric  $\text{LiTaO}_3$  (ASLT); (c)  $\text{LiNbO}_3$  decagonal nonlinear photonic quasi-crystal structure (DQC-LNB) and (d)  $\text{LiNbO}_3$  short-range ordered poled structures (SRO-LNB). For the cases depicted in graphs (a), (b) and (d) the X axis is horizontal and for the case (c)—vertical. The squares in graph (d) serve as guides to the eye and indicate the basic poling pattern azimuthally rotated at random angle.

cell with dimension  $a = 8.5 \mu\text{m}$ . The centers of rotation of each square form a two-dimensional regular square pattern with period  $b = 19.8 \mu\text{m}$  [see Fig. 2(d)-left]. All samples are Z-cut with thickness between 0.3–0.5 mm, and have all faces polished. We would like to stress that in this work we consider only the situation when the fundamental beam propagates along the polar (Z) axis which is different from reported elsewhere studies of Cerenkov SH radiation with fundamental wave propagating perpendicularly to the domain walls (inside the plane of modulation of nonlinearity) [16]–[18]. It should be mentioned that ideally, the periodically poled quadratic crystals should exhibit spatial modulation of the sign of nonlinearity only, while its refractive index should remain homogeneous. In reality the presence of domain walls at the boundaries of oppositely poled regions may induce change of the refractive index as well. In our samples such modulation of the refractive index was indeed observed. However, since it only led to a weak diffraction of the incident fundamental beam without

affecting conditions for the second harmonic generation we are not discussing it in the remainder of this work.

In the right column of Fig. 2 we show the Cerenkov SH emission rings recorded for different samples. It is clearly seen that in LiTaO<sub>3</sub> only one external ring is observed, while in LiNbO<sub>3</sub> two rings are visible. We measure the cone angles corresponding to the observed Cerenkov rings by comparing them with nonlinear diffraction that appears in the center [10]. For SRO-LNB sample the experimental cone angles for the Cerenkov SH radiation have values  $\beta_o = 40.3^\circ$  and  $\beta_e = 38.4^\circ$ , and for DQC-LNB the angles are  $\beta_o = 40.6^\circ$  and  $\beta_e = 38.8^\circ$ . For LiTaO<sub>3</sub> sample ASLT the experimental cone angle  $\beta = 32.3^\circ$ , while for RSLT sample is  $\beta = 32.6^\circ$ . We estimate the error of these values to  $\pm 0.4^\circ$ .

The immediate conclusion from these measurements is that the type of poled pattern does not influence the angular diameter of the SH Cerenkov ring. In the same time we have to point out that our attempt to observe visually the Cerenkov rings from single domain LiNbO<sub>3</sub> or stoichiometric LiTaO<sub>3</sub> samples using intensities up to the damage threshold failed. So, the intensity of the second harmonic Cerenkov rings is clearly enhanced by the domain structure of the sample.

As seen in Fig. 2, inside the rings, close to the center there is an additional second harmonic structure. This is a Raman–Nath type nonlinear diffraction at doubled frequency that in contrast to the Cerenkov rings is strongly dependent on the type of poled patterns. For example, for the ASLT sample [Fig. 2(b)–right] the Raman–Nath type nonlinear diffraction appears in form of rings with conical angles  $\alpha_m$  that satisfy the relation  $k_2 \sin \alpha_m = 2\pi/\Lambda$ , where  $m$  is integer. For one dimensional structures Raman–Nath type nonlinear diffraction was investigated in [10]. Results for the Raman–Nath nonlinear diffraction in two dimensional poled structures used in present work will be subject of separate publication.

The polarizations of the two Cerenkov rings in the LiNbO<sub>3</sub> samples [see Fig. 1(c)] have been determined to be as follows: for the internal ring—radial polarization (this means for each azimuthal angle the polarization is extraordinary) and for the external ring—the polarization is tangential (azimuthal), that corresponds to ordinary wave for each point of the ring. This is in accordance with the diagram in Fig. 1(a), (c). Since the input wave is always ordinary polarized the interaction responsible for the internal ring is  $E_2 - O_1O_1$  and the interaction responsible for the external ring is  $O_2 - O_1O_1$ . We have to note that such conical wave with radial or azimuthal polarization represents the far field of second harmonic Bessel beam inside the sample [19]. In the LiTaO<sub>3</sub> samples the Cerenkov second harmonic ring has elliptical polarization at each azimuthal angle, because it is formed by ordinary and extraordinary conical beams overlapping due to the low birefringence of the crystal.

Another important experimental observation is the azimuthal modulation of the Cerenkov rings. All rings exhibit two types of modulation: (i) sixfold modulation, and (ii) modulation with one or two maxima. In LiNbO<sub>3</sub> samples, the sixfold modulation of the SH emission is stronger than in stoichiometric LiTaO<sub>3</sub> samples ASLT and RSLT. Similar sixfold modulation was reported earlier in [12]. Here we prove that the origin of the sixfold modulation is indeed the hexagonal shape of the domains in LiNbO<sub>3</sub>

and stoichiometric LiTaO<sub>3</sub> samples. For the annular structure ASLT the origin of sixfold intensity modulation is different and will be discussed in the next section. The sixfold modulation does not depend on input polarization or input intensity and we found that it is directly connected with orientation of the axes X and Y of the sample. Rotation of the sample at some angle leads to rotation of sixfold structure by the same angle. This is illustrated in Fig. 2 where for one of the images (c), the sample is rotated at  $90^\circ$  angle with respect to the other three samples. The effect of sixfold modulation can be used as a fast purely optical method for discrimination between optical axes X and Y in poled structures.

The second type of azimuthal modulation seen in Cerenkov SH rings features one maximum (observed for the case of extraordinary Cerenkov SH rings in LiNbO<sub>3</sub> and in the Cerenkov SH rings in LiTaO<sub>3</sub>) or two maxima and minima (observed in the ordinary Cerenkov SH rings in LiNbO<sub>3</sub>). The azimuthal position of the maxima and minima depends on the orientation of input polarization. This effect was briefly discussed in [12] for an ASLT sample, where the azimuthal modulation is quite weak. Here we present new results for LiNbO<sub>3</sub> samples, where the modulation is much stronger. Fig. 2 offers direct comparison of this global modulation for the LiNbO<sub>3</sub> and LiTaO<sub>3</sub> samples. This difference in the modulation in the two types of samples will be discussed in the next section. The experimental results for the role of orientation of the input polarization on the position of maxima and minima of this second type of modulation of the ordinary and extraordinary Cerenkov SH rings obtained in SRO-LNB sample are shown in Fig. 3. The polarization angle (indicated in each graph) is measured counterclockwise from the X axis position of the sample that is vertical for the shown images. It is clearly seen that X and Y orientation of the input polarization leads to the same type of image but with mirror symmetry. In Fig. 3 it is seen that the sixfold modulation is fixed and does not depend on input polarization.

The experimental results on the effect of the input polarization on the position of the global maximum of the Cerenkov SH ring observed in the RSLT sample are shown in Fig. 4. While the observed dependence is the same as in Fig. 3, the contrast ratio between the intensities of the global maximum and minimum is lower due to different value for  $d_{32}/d_{22}$  ratio in LiTaO<sub>3</sub> crystal.

### III. COMPARISON WITH THE MODELS AND DISCUSSIONS

#### A. Cerenkov Conical Angles

Phase matching diagram of the process of generation of the Cerenkov rings at second harmonic frequency in birefringent crystals is shown in Fig. 1(a). The external conical angles  $\beta_o$ ,  $\beta_e$ , calculated using the following formulas:

$$\sin \beta_o = n_{2,o} \sin \cos^{-1}(2k_{1,o}/k_{2,o}), \quad (1)$$

$$\sin \beta_e = n_{2,e} \sin \cos^{-1}(2k_{1,o}/k_{2,e}) \quad (2)$$

are found to be as follows: (a) For LiNbO<sub>3</sub> samples  $\beta_o = 40.64^\circ$  and  $\beta_e = 38.78^\circ$ . These values are in excellent agreement with the experimental data reported in the previous section. (b) For stoichiometric LiTaO<sub>3</sub> the calculated values with (1), (2) are

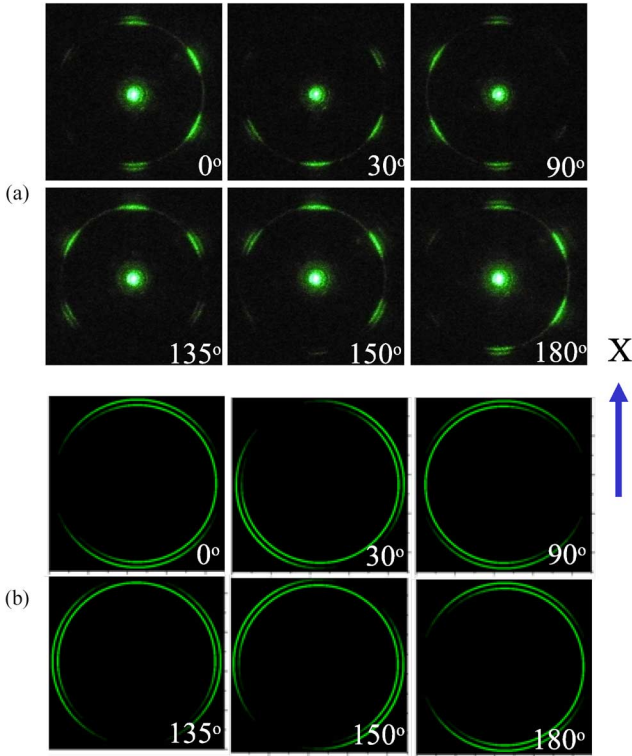


Fig. 3. (a) Experimental images showing the effect of the input polarization on the Cerenkov SH rings in SRO-LNB sample. The input polarization angle is measured counterclockwise from the axis X (vertical). (b) Theoretically predicted azimuthal intensity modulation in the SH ring for different angles of the input polarization in  $\text{LiNbO}_3$ .

$\beta_o = 32.95^\circ$  and  $\beta_e = 32.2^\circ$ . We used Sellmeier coefficients recently published in [20]. The angular difference  $\beta_o - \beta_e$  between the conical angles of the ordinary and the extraordinary rings in the cases of ASLT and RSLT samples is too small and remained not resolved in the experiment. For the RSLT sample the agreement between the experimentally determined angle  $\beta = 32.6^\circ$  and the calculated average of ordinary and extraordinary angle values  $\beta = 32.57^\circ$  is also very good.

### B. Azimuthal Intensity Modulation of the Rings Due to $d_{\text{eff}}^{(2)}$

As we pointed out, the recorded Cerenkov rings have two types of azimuthal modulation—sixfold modulation and additional modulation with one or two maxima. The modulation with one or two maxima can be explained considering the effective quadratic nonlinearity built on the base of the polarization properties of the  $d^{(2)}$  tensor. As we mentioned above, the inner Cerenkov ring is generated in  $E_2 - O_1O_1$  process and the outer ring is  $O_2 - O_1O_1$ . As a result, the effective nonlinearities of these two parametric processes should be different and can be written as [12], [21]:

$$d_{\text{eff}}^{(o)}(\varphi, \gamma) = d_{\text{yyy}} \cos(\varphi + 2\gamma), \quad (3)$$

$$d_{\text{eff}}^{(e)}(\varphi, \gamma, \theta) = d_{\text{yyy}} \cos \theta_e \sin(\varphi + 2\gamma) + d_{\text{zyy}} \sin \theta_e, \quad (4)$$

where  $\varphi$  is the azimuthal angle measured counterclockwise from the X axis,  $\theta$  is the angle of the direction of Cerenkov SH radiation inside the crystal with respect to crystal axis Z, and  $\gamma$  is the azimuthal angle that defines the polarization of the input

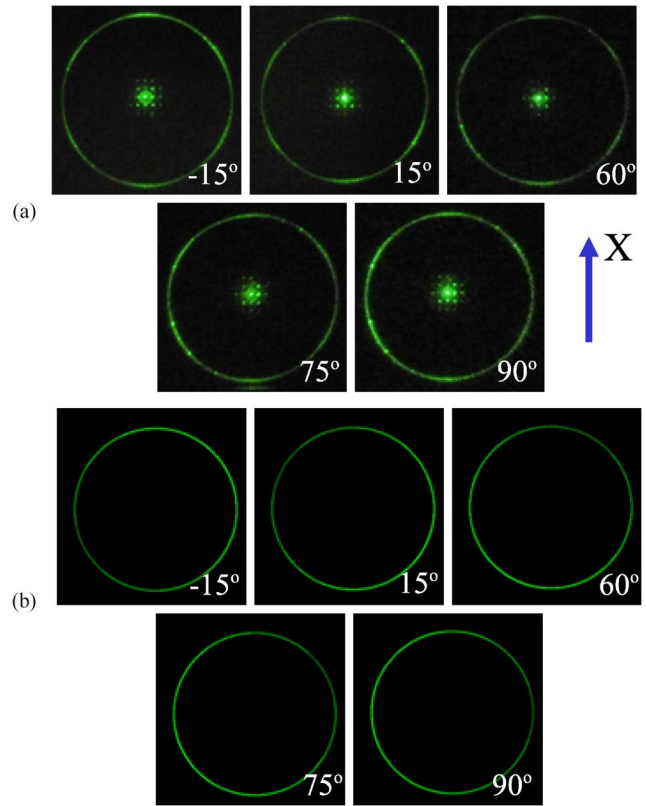


Fig. 4. Experimental images showing the role of orientation of input polarization on the Cerenkov SH rings obtained in RSLT sample. The polarization angle is measured counterclockwise from axis X (vertical). (b) Theoretically predicted azimuthal intensity modulation in the SH ring for different angles of the input polarization in  $\text{LiTaO}_3$  sample.

beam ( $\gamma = 0$  for input polarization directed along X axis). In the undepleted pump regime of SHG, the intensity of the ordinary and extraordinary SH Cerenkov rings is proportional to  $[d_{\text{eff}}^{(o)}]^2$  or to  $[d_{\text{eff}}^{(e)}]^2$ , respectively. Hence, the dependence on the input polarization is defined by the angle  $\gamma$ . In Fig. 3(b) we show the simulations of the intensity distributions of the SH rings according to  $I_2^{(o,e)}(\varphi, \gamma) = A[d_{\text{eff}}^{(o,e)}(\varphi, \gamma)]^2$ , for several angles of the input polarization. It can be seen that the ordinary SH ring has two intensity maxima and the extraordinary SH ring has only one intensity maximum. In these theoretical figures we did not include the sixfold modulation that has a different physical background and will be discussed in the next subsections. As seen from the comparison of Fig. 3(a) and Fig. 3(b) the  $[d_{\text{eff}}^{(o,e)}]$  approach describes very well the role of input polarization. In the simulations shown in Fig. 3(b) we use ratio of the two components of the tensor of second order nonlinearity  $d_{32}/d_{22} = -3.9$  [22], [23].

The situation is different for stoichiometric  $\text{LiTaO}_3$  samples. The two rings are not resolved and then the SH intensity observed in the experiment should be described simply by the sum

$$I_2(\varphi, \gamma) = I_2^{(o)}(\varphi, \gamma) + I_2^{(e)}(\varphi, \gamma). \quad (5)$$

In Fig. 4(a) and Fig. 4(b) we compare the experimental rings obtained with the RSLT sample with the theoretical predictions (Eq. (5)). In the simulations shown in Fig. 4(b) we use the ratio

of the two nonlinear components in LiTaO<sub>3</sub>  $d_{32}/d_{22} = -0.59$  [24]. In principle accurate measurement of the maximal and minimal intensity of the Cerenkov SH ring will allow independent experimental determination of the ratio  $d_{32}/d_{22}$  and its comparison with other available in the literature data, as in [20].

### C. Azimuthal Intensity Modulation of the Rings Due to Hexagonal Shape of the Individual Domains

Compared with  $d_{\text{eff}}^{(2)}$ -mediated modulation of the Cerenkov SH rings, the sixfold modulation needs more thorough interpretation. It was suggested in [12] that there is connection between the hexagonal shape of the individual ferroelectric domains and the sixfold modulation of the emission rings. Here we prove that, indeed the origin of the sixfold modulation is the hexagonal shape of the ferroelectric domains in LiNbO<sub>3</sub> and stoichiometric LiTaO<sub>3</sub> samples. Moreover, as seen in Figs. 2–4, in LiNbO<sub>3</sub> samples the sixfold modulation is deeper than in stoichiometric LiTaO<sub>3</sub> samples. This is because the LiNbO<sub>3</sub> samples have bigger density of hexagon-shaped domains than the stoichiometric LiTaO<sub>3</sub> samples. For the annular sample ASLT [Fig. 2(b)-left] we do not have individual hexagon-shaped domains. There the origin of the sixfold intensity modulation is different and will be discussed in the next subsection.

The association of Cerenkov SH emission pattern with the shapes of the ferroelectric domains (nonlinear motifs) is constituted through the structure's reciprocal vectors. It is known that the output intensity of a QPM interactions in nonlinear photonic structures is proportional to the square of the Fourier coefficient  $g_{mn}$ . As shown in [25] and [26], when a nonlinear process is phase matched by a reciprocal lattice vector  $G_{mn}$  in an infinite two-dimensional periodic lattice, this coefficient is given by the Fourier transform of the nonlinear motif at a spatial frequency  $G_{mn}/(2\pi)$ , divided by the unit cell area.

In most of the publications that study the two dimensional nonlinear photonic structures, it is assumed that the individual domains are of circular transverse profile and consequently its Fourier spectrum  $\{g, \mathbf{G}\}$  is represented by the first order Bessel function, which is radially symmetric and isotropic in two-dimensional reciprocal space. Recently rectangular [25], triangular and hexagonal [26] domains were studied. The hexagonal motif is particularly relevant to this work, since in all our samples we always deal with a hexagon-shaped domains [see Fig. 2(c)-left] owing to the crystal 3m symmetry [27], [28]. As a result, the actual Fourier spectrum  $\{g, \mathbf{G}\}$  reflects the hexagonal symmetry of the domains. Such nonuniform, hexagonal distribution of vectors  $\mathbf{G}$  will have a very little effect on the first order QPM interactions because the domain size (with radius  $\approx 3 \mu\text{m}$ ) is much smaller than  $\chi^{(2)}$  modulation ( $\approx 10 \mu\text{m}$ ). However it will contribute toward fulfillment of the full vectorial phase matching condition for the Cerenkov SH radiation for which the required reciprocal vectors are of rather large magnitude. As a consequence at almost exact fulfillment of the full phase matching, the SH intensity of the Cerenkov ring is expected to be strongly enhanced along the six directions representing the axes of a hexagon.

This hypothesis was firstly verified by measuring linear diffraction images of etched SRO-LNB sample [see Fig. 5(b)].

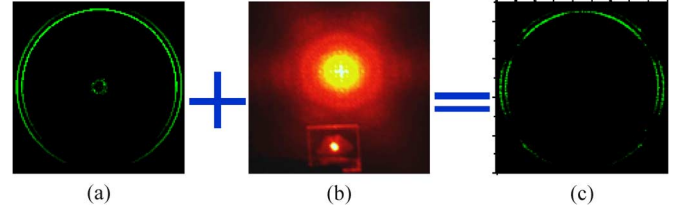


Fig. 5. (a) Theoretical prediction for the azimuthal intensity modulation of the Cerenkov ring caused solely by the polarization properties of  $d_{\text{eff}}^{(2)}$  in case of LiNbO<sub>3</sub> samples. (b) Experimentally observed linear light diffraction in SRO-LNB sample indicating a sixfold symmetry in the density of reciprocal lattice vectors caused by the hexagonal domain shape. (c) Theoretically predicted light intensity modulation in the Cerenkov SH ring obtained by taking into account both, domain hexagonal shape and polarization properties of the effective nonlinearity  $d_{\text{eff}}^{(2)}$ .

The linear diffraction pattern with hexagonal symmetry directly indicates the density of the available reciprocal lattice vectors for phase matching. Secondly, it is supported by the theoretical simulations. For the structures that consist of hexagonal domains (as RSLT, DQC-LNB, and SRO-LNB samples) important is only the distribution  $g(\varphi)$  of the Fourier coefficients of those reciprocal vectors whose magnitude is equal or close to the phase mismatch of Cerenkov rings, namely for  $\Delta k = k_2 \sin \theta$ . To account for this mismatch we introduce in the expression for the SH intensity the  $\text{sinc}^2$  function:

$$I_2^{(o,e)}(\varphi) = A \left[ d_{\text{eff}}^{(o,e)}(\varphi) g(\varphi) L \right]^2 \left[ \frac{\sin \left[ (|G| - \Delta k) L / 2 \right]}{(|G| - \Delta k) L / 2} \right]^2 \quad (6)$$

where  $A$  is a constant and  $L$  is the thickness of the sample.

The image in Fig. 5(c) is obtained by plotting the formula (6) and taking into account both the effect of hexagonal intensity modulation and the polarization properties of the effective second order nonlinearity. It can be clearly seen that the sixfold intensity modulation of the Cerenkov ring closely reflects the actual experimental observations shown in Figs. 2–4.

### D. Azimuthal Intensity Modulation of the Cerenkov Rings in ASLT Sample Due to the Properties of the Poled Annular Domains

In case of the annular structure in the ASLT the origin of the azimuthal intensity modulation is even more interesting. As shown in Fig. 2, for the structures such as RSLT and DQC-LNB the sixfold modulation is only visible in the Cerenkov SH rings. In the ASLT sample however such modulation affects the whole intensity distribution of the SH, including both, the Cerenkov rings and the centrally located emission region, where at least the first two Raman–Nath nonlinear diffraction orders can be seen [see Fig. 2(b)-right].

As follow from the relation between the magnitude (length) of reciprocal vectors and the domain size, only the reciprocal vectors with magnitude equal or larger than  $\pi/3 \mu\text{m}$  can be expected to be influenced by the hexagonal shape of the domains. Consequently, the sixfold intensity modulation only occurs to the Cerenkov rings. For the ASLT sample, there are no such small hexagonal shaped domains. However, by careful inspection of the poled annular rings in Fig. 2(b)-left, we found out that the domain rings exhibit tendency to merge roughly every

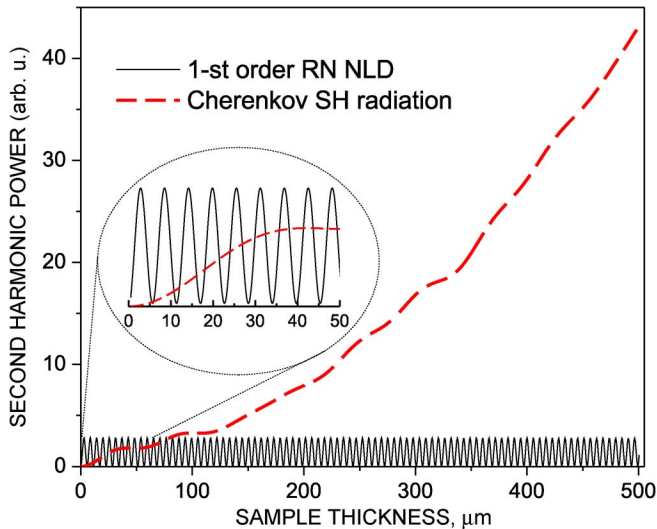


Fig. 6. Simulation results with split step Fourier method for the dependence of the intensity of the Cerenkov second harmonic on the thickness of the LiNbO<sub>3</sub> sample when propagation direction coincides with the optical axis Z.

60° hence introducing again sixfold azimuthal modulation of the poling pattern.

This phenomenon was observed before and explained as a result of the spatial anisotropy of the velocity of domain growth, caused by the larger tangential poling electric field components and the smaller depolarization and domain-wall energies in particular spatial directions [27], [29]. Therefore, instead of concentric domains in form of rings, the ASLT sample is actually composed in some sense of concentric domains in form of hexagonally deformed rings. As a result, the Fourier spectrum of the structure (reciprocal vectors) exhibits again hexagonal symmetry in the entire reciprocal space, i.e., long and short reciprocal vectors are affected. Subsequently, the hexagonal intensity modulation occurs in all the SH emission patterns in the ASLT—the Cerenkov ring and the Raman–Nath nonlinear diffraction, agreeing well with our experimental observations.

#### E. Dependence of Ring Intensity on Sample Thickness

The dependence of the intensity of the SH on the length of the nonlinear media is an important characteristic that is difficult to address experimentally. We simulated the generation of the Cerenkov second harmonic radiation using the split-step Fourier method and assuming undepleted propagation of the fundamental beam through the nonlinear crystal. The pump beam creates nonlinear polarization source term that is used to generate second harmonic wave. The 0.5 mm thick nonlinear photonic structure was divided into slabs of 1 μm thickness, and every Z plane in the crystal was split into 0.25 × 0.25 μm elements. The second harmonic wave was convolved in each slab with the impulse response of a free-space slab. The resulting dependence of SH intensity on the distance traveled by the fundamental beam is shown in Fig. 6.

The simulation results obtained for the case of LiNbO<sub>3</sub> sample with one-dimensional nonlinear grating, when the fundamental beam is directed along the Z axis, show that the Cerenkov SH radiation, which is defined by the longitudinal

phase matching condition only, is coherently growing through the sample like a fully phase matched process. In contrast, the second harmonic intensity of the Raman–Nath nonlinear diffraction (RN NLD), seen in the center of the images, oscillates with the period  $2\pi/(k_2 \cos \alpha_1 - 2k_1)$  ( $\alpha_1$  is diffraction angle of first order RN NLD) like the non-phase matched process, regardless of the fact that for this Raman–Nath type nonlinear diffraction the transverse phase matching is fulfilled [10].

We demonstrated above that the Cerenkov second harmonic radiation is enhanced by the poled structure. The Fourier spectrum of both the poled structure and the individual domains is so rich that almost continuous set of reciprocal vectors is available in certain directions in the X-Y plane. This compensates the mismatch  $\Delta k$  for the Cerenkov SHG process such that it becomes a fully phase matched process, thus enhancing its efficiency. However, the direction of the Cerenkov SH radiation remains defined solely by the longitudinal phase matching condition  $k_2 \cos \theta = 2k_1$ .

#### IV. CONCLUSION

We have studied experimentally the Cerenkov-type second-harmonic generation in several different (ordered and partially disordered) two-dimensional nonlinear photonic structures. We have demonstrated that the nonlinearity modulation does not change the direction of the Cerenkov second-harmonic emission defined by the longitudinal phase matching condition. However the modulation of the quadratic response enhances greatly the Cerenkov emission converting it in some cases to a fully phase-matched process.

We believe that the effect of the nonlinear photonic structure on the intensity of the Cerenkov second-harmonic emission can have several possible applications, including nondestructive testing of the poled structure, second-harmonic microscopy, single-shot reconstruction of femtosecond pulses [30], efficient cascaded third-harmonic generation [31], and the study of dispersion properties of nonlinear materials.

#### REFERENCES

- [1] A. Zembrod, H. Puell, and J. Giordmaine, "Surface radiation from nonlinear optical polarization," *Opto-electronics*, vol. 1, no. 1, pp. 64–66, 1969.
- [2] J. V. Jelley, *Cerenkov Radiation*. New York: Pergamon Press, 1958.
- [3] V. Vacaitis, "Cerenkov-type phase matching in bulk KDP crystal," *Opt. Commun.*, vol. 209, pp. 485–490, 2002.
- [4] A. A. Kaminskii, H. Nishioka, K. Ueda, W. Odajima, M. Tateno, K. Sasaki, and A. V. Butashin, "Second-harmonic generation with Cerenkov-type phase matching in a bulk nonlinear LaBGeO<sub>5</sub> crystal," *Quantum Electron.*, vol. 26, no. 5, pp. 381–382, 1996.
- [5] P. K. Tien, R. Ulrich, and R. J. Martin, "Optical second harmonic generation in form of coherent cerenkov radiation from a thin-film waveguide," *Appl. Phys. Lett.*, vol. 17, no. 10, pp. 447–449, 1970.
- [6] K. Hayata, K. Yanagawa, and M. Koshiba, "Enhancement of the guided-wave second-harmonic generation in the form of Cerenkov radiation," *Appl. Phys. Lett.*, vol. 56, no. 3, pp. 206–208, 1990.
- [7] M. J. Li, M. de Micheli, Q. He, and D. B. Ostrowsky, "Cerenkov configuration second harmonic generation in proton-exchanged lithium niobate guides," *IEEE Journal of Quantum Electronics*, vol. 26, no. 8, pp. 1384–1393, 1990.
- [8] V. Berger, "Nonlinear photonic crystals," *Phys. Rev. Lett.*, vol. 81, pp. 4136–4139, 1998.
- [9] A. Fragemann, V. Pasiskevicius, and F. Laurell, "Second-order nonlinearities in the domain walls of periodically poled KTiOPO," *Appl. Phys. Lett.*, vol. 85, no. 3, pp. 375–377, 2004.

- [10] S. M. Saltiel, D. N. Neshev, W. Krolikowski, A. Arie, O. Bang, and Y. S. Kivshar, "Multi-order nonlinear diffraction in frequency doubling processes," *Opt. Lett.*, vol. 34, no. 6, pp. 848–850, 2009.
- [11] D. Kasimov, A. Arie, E. Winebrand, G. Rosenman, A. Bruner, P. Shaier, and D. Eger, "Annular symmetry nonlinear frequency converters," *Opt. Express*, vol. 14, no. 20, pp. 9371–9376, 2006.
- [12] S. M. Saltiel, D. N. Neshev, W. Krolikowski, R. Fischer, A. Arie, and Yu S. Kivshar, "Generation of second-harmonic conical waves via nonlinear Bragg diffraction," *Phys. Rev. Lett.*, vol. 100, no. 10, pp. 103902(1)–103902(4), 2008.
- [13] Y. Sheng, J. Dou, B. Cheng, and D. Zhang, "Effective generation of red-green-blue laser in a two-dimensional decagonal photonic superlattice," *Appl. Phys. B*, vol. 87, no. 4, pp. 603–606, 2007.
- [14] Y. Sheng, J. Dou, J. Li, D. Ma, B. Cheng, and D. Zhang, "Broadband efficient second harmonic generation in media with a short-range order," *Appl. Phys. Lett.*, vol. 91, pp. 011101(1)–011101(3), 2007.
- [15] Y. Sheng, "Cascaded third-harmonic generation in a single short-range-ordered nonlinear photonic crystal," *Opt. Lett.*, vol. 34, no. 5, pp. 656–658, 2009.
- [16] G. Y. Wang and E. M. Garmire, "High-efficiency generation of ultrashort second-harmonic pulses based on the Cerenkov geometry," *Opt. Lett.*, vol. 19, pp. 254–256, 1994.
- [17] Y. Zhang, Z. Qi, W. Wang, and S. N. Zhu, "Quasi-phase-matched Cerenkov second-harmonic generation in a hexagonally poled LiTaO<sub>3</sub> waveguide," *Appl. Phys. Lett.*, vol. 89, no. 1, pp. 171113(1)–171113(3), 2006.
- [18] Y. Zhang, Z. D. Gao, Z. Qi, S. N. Zhu, and N. B. Ming, "Nonlinear Cerenkov radiation in nonlinear photonic crystal waveguides," *Phys. Rev. Lett.*, vol. 100, no. 16, pp. 163904(1)–163904(4), 2008.
- [19] S. M. Saltiel, W. Krolikowski, D. N. Neshev, and Yu S. Kivshar, "Generation of Bessel beams by parametric frequency doubling in annular nonlinear periodic structures," *Opt. Express*, vol. 15, no. 7, pp. 4132–4138, 2007.
- [20] I. Dolev, A. Ganany-Padowicz, O. Gayer, A. Arie, J. Mangin, and G. Gadret, "Linear and nonlinear optical properties of MgO : LiTaO<sub>3</sub>," *Appl. Phys. B*, vol. 96, no. 2–3, pp. 423–432, 2009.
- [21] S. M. Saltiel, D. N. Neshev, R. Fischer, W. Krolikowski, A. Arie, and Yu S. Kivshar, "Generation of second-harmonic Bessel beams by transverse phase-matching in annular periodically poled structures," *Japanese Journal of Applied Physics*, vol. 47, no. 8, pp. 6777–6783, 2008.
- [22] A. Ganany, A. Arie, and S. M. Saltiel, "Quasi-phase matching in LiNbO<sub>3</sub> using nonlinear coefficients in the XY plane," *Appl. Phys. B*, vol. 85, pp. 97–100, 2006.
- [23] D. N. Nikogosyan, *Nonlinear Optical Crystals: A complete Survey*. : Springer Science+Business Media, Inc, 2005.
- [24] F. Charra and G. G. Gurzadyan, *Nonlinear Dielectric Susceptibilities*, D. F. Nelson, Ed. Berlin: Springer, 2000.
- [25] A. Arie, N. Habshoosh, and A. Bahabad, "Quasi phase matching in two-dimensional nonlinear photonic crystals," *Optical and Quantum Electronics*, vol. 39, no. 4–6, pp. 361–375, 2007.
- [26] A. Arie, A. Bahabad, and N. Habshoosh, "Nonlinear interactions in periodic and quasi-periodic nonlinear photonic crystals," in *Ferroelectric Crystals for Photonic Applications*, P. Ferraro, S. Grilli, and P. De Natale, Eds. Berlin Heidelberg: Springer Verlag, 2009, ch. 10, pp. 259–284.
- [27] Y. Sheng, T. Wang, B. Ma, E. Qu, B. Cheng, and D. Zhang, "Anisotropy of domain broadening in periodically poled lithium niobate crystals," *Appl. Phys. Lett.*, vol. 88, no. 4, pp. 041121(1)–041121(3), 2006.
- [28] G. Rosenman, Kh. Garb, and A. Skliar, "Domain broadening in quasi-phase-matched nonlinear optical devices," *Appl. Phys. Lett.*, vol. 73, no. 7, pp. 865–867, 1998.
- [29] T. Wang, B. Ma, Y. Sheng, P. Ni, B. Cheng, and D. Zhang, "Large angle acceptance of quasi-phase-matched second harmonic generation in a homocentrally poled LiNbO<sub>3</sub>," *Opt. Commun.*, vol. 252, pp. 397–401, 2005.
- [30] S. J. Holmgren, C. Canalias, and V. Pasiskevicius, "Ultrashort single-shot pulse characterization with high spatial resolution using localized nonlinearities in ferroelectric domain walls," *Opt. Lett.*, vol. 32, no. 11, pp. 1545–1547, 2007.
- [31] N. Voloch, T. Ellenbogen, and A. Arie, "Radially symmetric nonlinear photonic crystals," *J. Opt. Soc. Am.*, vol. 26, no. 1, pp. 42–49, 2009.



**Solomon Mois Saltiel** was born in Sofia, Bulgaria. He received the M.S. and Ph.D. degrees from Moscow State University, Moscow, U.S.S.R., in the field of nonlinear optics in 1973 and 1976, respectively.

In 1976, he joined the Faculty of Physics, Sofia University, as an Associate Professor. In 1995 he received the position of Professor. He was with the University of California, Irvine, in 1988 and 1989. Solomon Saltiel's research interests included nonlinear optics and laser spectroscopy.

Prof. Saltiel was a member of the Optical Society of America and the Union of Physicists in Bulgaria. In 2005 he was elected as Corresponding member of Bulgarian Academy of Sciences.



**Yan Sheng** was born in China in 1979. She received the B.S. and M.S. degrees in physics and optics from the Capital Normal University, Beijing, China, in 1997 and 2001, respectively, and the Ph.D. degree in optical physics from the Institute of Physics, Chinese Academy of Science, Beijing, China, in 2007. For her Ph.D. thesis with honor, she studied broadband and enhanced optical parametric processes in two-dimensional nonlinear photonic crystals.

Since then, she has been a Postdoctoral Fellow in the Max Planck Institute for Polymer Research, Mainz, Germany, where she has been working on the cascaded second-order nonlinear interactions in different poled nonlinear optical materials.



**Noa Voloch** received the B.Sc. degree from the Technion-Israel Institute of Technology, Haifa, Israel, in 2004, and the M.Sc. degree from Tel-Aviv University, Tel-Aviv, Israel, in 2007, both in physics. She is currently pursuing the Ph.D. degree in electrical engineering at Tel-Aviv University.



**Dragomir N. Neshev** received the Ph.D. degree in physical sciences from Sofia University, Bulgaria, in 1999.

Since then, he has worked in the field of nonlinear optics, gaining experience at several research Centres and countries. In 2002, he took up an appointment at the Australian National University and is currently a Fellow with the Nonlinear Physics Centre. Dr. Neshev now leads the experimental photonics group at Nonlinear Physics Centre, focused on research in nonlinear nanophotonics. His interests include light propagation in nonlinear periodic dielectric and metallic structures, nonlinear singular optics, and harmonics generation.



**Wieslaw Krolikowski** received the Ph.D. degree in physics from the Institute of Physics, Polish Academy of Sciences, Warsaw, in 1988, and the D.Sc. (habilitation) degree in physics from the Warsaw University of Technology, Warsaw, Poland, in 2001. From 1988 to 1991 he was a Research Associate at Tufts University, Medford MA. Since 1992 he has been with the Laser Physics Centre, Australian National University in Canberra, where he is currently a Professor. His research interest includes experimental and theoretical aspects of light

localization and optical solitons, parametric processes, nonlinear dynamics, photorefractive nonlinear optics, fiber and integrated optics. Dr. Krolikowski is a member of the Australian Optical Society and a Fellow of the Optical Society of America.



**Ady Arie** (M'96–SM'99) received the B.Sc. degree in mathematics and physics from the Hebrew University of Jerusalem, Israel, in 1983, and the M.Sc. degree in physics and the Ph.D. degree in engineering from Tel-Aviv University, Tel-Aviv, Israel, in 1986 and 1992, respectively.

Between 1991 and 1993, he was a Wolfson and Fulbright Postdoctoral Scholar in the group of Prof. Robert L. Byer at Ginzton Laboratory, Stanford University, Stanford, CA. In 1993, he joined the Department of Physical Electronics, School of Electrical Engineering in the Faculty of Engineering, Tel-Aviv University. Since 2006, he has been a Professor of electrical engineering. His research in recent years is in the areas of nonlinear optics and high resolution spectroscopy.

Prof. Arie is a Chair of the Israel Section of IEEE-LEOS, Vice President of the Israeli Lasers and Electro-Optic Society, and a Member of the Optical Society of America.



**Kaloian Koynov** received the M.Sc. and Ph.D. degrees in physics from Sofia University, Sofia, Bulgaria, in 1993 and 1997, respectively.

After a postdoctoral year in the Institute for Fundamental Electronics, University Paris Sud, France, in 2000 he joined the Max Planck Institute for Polymer Research in Mainz, Germany as a post-doc and EU Marie Curie Fellow. Since 2006, he has been a Project Leader in the same institute. His research interests fall in the broad areas of photonics, material science and polymer physics.

Dr. Koynov is a member of the Optical Society of America and the Union of Physicists in Bulgaria.



**Yuri S. Kivshar** received the Ph.D. degree in 1984 from the Institute for Low Temperature Physics and Engineering (Ukraine) for research in nonlinear waves and solitons.

After postdoctoral and visiting research positions at different centres in the USA and Europe, he joined the Australian National University in 1993, where he is currently Professor and Australian Research Council Federation Fellow. In 2002, he founded Nonlinear Physics Center. His research focuses on nonlinear optics, photonics, and application of nonlinear physics to all-optical technologies.

Dr. Kivshar was a recipient of many awards, including the International Pnevmatikos Prize in Nonlinear Science (1995), Pawsey Medal (1998), Boas Medal (2005) and Lyle Medals of the Australian Academy of Science (2007). He is a Fellow of the Optical Society of America, Fellow of the American Physical Society, and Fellow of the Australian Academy of Science.